

## Network Domain Structure in Viscoelastic Phase Separation

Takashi Taniguchi and Akira Onuki

*Department of Physics, Kyoto University, Kyoto 606-01, Japan*

(Received 9 September 1996)

By solving a viscoelastic model of polymer solutions in two dimensions, we demonstrate that polymer-rich regions can form a spongelike network in deeply quenched cases. In late stages the velocity field is suppressed because the network supports stress and is rigid. As a result the domain size grows as  $t^{1/3}$ . In an early stage the polymer-rich regions are shrunken due to desorption of solvent, whereas in late stages they are elastically expanded perpendicularly to the interface in regions with relatively small curvature. The viscoelastic stress then cancels the stress due to the surface tension and stabilizes the network structure for a long time. [S0031-9007(96)01792-9]

PACS numbers: 61.25.Hq, 64.75.+g

Recently a great number of phase separation experiments have been performed on polymeric systems [1]. While most of them can be understood in the light of simple dynamic models for usual fluids, some experiments have revealed unusual influence of viscoelasticity peculiar to polymers. Among them Tanaka [2] examined in detail a spongelike network structure composed of thin polymer-rich regions by deeply quenching semidilute polymer solutions into an unstable temperature region. Such patterns were already observed by Aubert [1] and by Song and Torkelson [1]. There, holes of solvent appear in an early stage after an incubation time and grow until polymer-rich regions become thin to form a spongelike network. The solvent regions are droplets enclosed by the network even if their volume fraction is considerably larger than that of the network. This structure coarsens in time and ultimately breaks into disconnected polymer-rich domains. Tanaka also observed the same network formation in a polymer blend in which one phase is close to glass transition [3]. Therefore a network appears generally when the two phases have very different viscoelastic properties. The aim of this paper is hence to numerically investigate the role of viscoelasticity in producing such a network pattern in late stage spinodal decomposition in polymer solutions.

We present a dynamic model of a semidilute polymer solution in which the polymer volume fraction  $\phi$  satisfies  $\phi > \phi_c$  and  $\phi \ll 1$ ,  $\phi_c = N^{-1/2}$  being the critical volume fraction and  $N$  being the polymerization index [4]. We introduce a tensor variable  $\vec{W}$ , called the conformation tensor, to represent chain deformations. In terms of  $\phi$  and  $\vec{W} = \{W_{ij}\}$ , the free energy is given by [5–8]

$$F = \int dr \left[ f + \frac{1}{2} C |\nabla \phi|^2 + \frac{1}{4} G \sum_{ij} (\delta W_{ij})^2 \right]. \quad (1)$$

Here  $f \cong (k_B T / v_0) [\phi \ln \phi / N + (\frac{1}{2} - \chi) \phi^2 + \frac{1}{6} \phi^3]$  is the Flory-Huggins free energy density [4], where  $v_0$  is the volume of a monomer and  $\chi$  is the interaction parameter dependent on the temperature. In the second term  $C(\phi) \propto 1/\phi$  from the scaling theory. The last term of (1) is

the elastic energy of the network,  $G(\phi)$  being the shear modulus. For simplicity we assume that the deviation of  $W_{ij}$  from the equilibrium value  $\delta_{ij}$  (= the unit tensor) is small, so the elastic free energy is bilinear in  $\delta W_{ij} = W_{ij} - \delta_{ij}$  in our model. The motion of  $W_{ij}$  is determined by the polymer velocity  $\mathbf{v}_p$  and its simplest dynamic equation is of the form [9]

$$\frac{\partial}{\partial t} \vec{W} + (\mathbf{v}_p \cdot \nabla) \vec{W} = \vec{D} \cdot \vec{W} + \vec{W} \cdot \vec{D}^T - \frac{1}{\tau} (\vec{W} - \vec{1}), \quad (2)$$

where  $\vec{D} = \{\partial v_{pi} / \partial x_j\}$  is the gradient tensor of the polymer velocity  $\mathbf{v}_p$  and  $\vec{D}^T$  is its transposed tensor. The relaxation time  $\tau(\phi)$  is very long in the semidilute region. From (1) and (2) we may calculate free energy changes against infinitesimal motion of the network to obtain the network stress

$$\sigma_p = G \vec{W} \cdot (\vec{W} - \vec{1}). \quad (3)$$

For motions of polymers much slower than  $\tau$ , we have  $W_{ij} - \delta_{ij} \cong \tau(D_{ij} + D_{ji})$  and obtain the Newtonian viscosity  $\eta_p = G\tau$ , which is supposed to be much larger than the solvent viscosity  $\eta_0$  in the semidilute case. For rapid motions, on the other hand, our system behaves as a gel and  $\delta W_{ij}$  is nearly equal to the strain tensor of the displacement  $\mathbf{u}_p$  which is the time integral of  $\mathbf{v}_p$ .

The solvent velocity  $\mathbf{v}_s$  and the polymer velocity  $\mathbf{v}_p$  are different when the diffusion is taking place. The volume fraction is convected by  $\mathbf{v}_p$  as

$$\frac{\partial}{\partial t} \phi = -\nabla \cdot (\phi \mathbf{v}_p). \quad (4)$$

For slow motions we may neglect the acceleration of the average velocity  $\mathbf{v} = \phi \mathbf{v}_p + (1 - \phi) \mathbf{v}_s$  to obtain

$$\eta_0 \nabla^2 \mathbf{v} = [C(\nabla \phi)(\nabla \phi) - \nabla \cdot \sigma_p]_{\perp}, \quad (5)$$

where  $[\dots]_{\perp}$  denotes taking the transverse part. For simplicity we are assuming that the mass densities of the pure polymer and solvent are the same and the fluid is incompressible, so  $\nabla \cdot \mathbf{v} = 0$  holds. Then  $\mathbf{v}$  may be

expressed in terms of  $\phi$  and  $\vec{W}$  and calculated using the FFT scheme. Furthermore, on the assumption that the network stress acts on the polymer and not directly on the solvent [10], a two fluid model [5–8,10,11] gives the relative velocity  $\mathbf{w} = \mathbf{v}_p - \mathbf{v}_s$  as

$$\zeta \mathbf{w} = -\phi \nabla \frac{\delta F}{\delta \phi} + \nabla \cdot \vec{\sigma}_p + \frac{1}{4} G \nabla \sum_{ij} (\delta W_{ij})^2, \quad (6)$$

where  $\zeta(\phi)$  is the friction coefficient of order  $6\pi\eta_0 b^{-2}\phi^2$ ,  $b$  being the monomer size. The last two terms in (6) show how diffusion is influenced by viscoelasticity. We can see that stress imbalance ( $\nabla \cdot \vec{\sigma}_p \neq 0$ ) produces diffusion. This form of  $\mathbf{w}$  was originally derived for gels to analyze dynamic light scattering [12] and recently used for sheared polymer solutions [11]. This effect is called the stress-diffusion coupling and is generally present in viscoelastic two component systems, giving rise to non-exponential decay in dynamic light scattering [10] and shear-induced composition fluctuations [7,8,10,11]. Its effects on early stage spinodal decomposition have also been discussed [13,14]. As the self-consistency condition of our model, if the system is closed, we can check  $dF/dt \leq 0$  from (1)–(6) for any disturbances. This condition assures that the system tends to a homogeneous equilibrium state as  $t \rightarrow \infty$  if it is closed.

We numerically integrate (2) and (4) using  $\mathbf{v}_p \equiv \mathbf{v} + \mathbf{w}$  on a  $256 \times 256$  square lattice under the periodic boundary condition. Note that  $\mathbf{v}$  and  $\mathbf{w}$  have been expressed in terms of  $\phi$  and  $W_{ij}$ . We measure space and time in the units of  $\ell = (NC_0)^{1/2}/4$  and  $\tau_0 = (v_0 N^{1/2}/k_B T)(\zeta/\phi^2)\ell^2$ , where  $C(\phi)$  in (1) is set equal to  $(k_B T/v_0)C_0/\phi$ . The grid size is  $\Delta x = 1$ , so the space region is  $0 < x, y < 256$ . The time step is  $\Delta t = 10^{-3}$ . In the initial state at  $t = 0$ ,  $\Phi(x, y, t)$  at each lattice point is a Gaussian random number with  $\langle (\Phi - \langle \Phi \rangle)^2 \rangle = 0.01$ . For  $t > 0$  we set  $(1 - 2\chi)N^{1/2} = 4.25$ , for which  $\Phi = 5.86$  in the polymer-rich phase and  $\Phi = 0.0026$  in the solvent-rich phase on the coexistence curve. Hereafter we write  $\Phi = \phi/\phi_c$ . In this final polymer-rich phase, let  $\xi$  and  $D_{co}$  be the thermal correlation length ( $\sim$  the interface width) and the cooperative diffusion constant [4], respectively. Then we obtain  $\ell = 0.81\xi$  and  $\tau_0 = 1.16\xi^2/D_{co}$ . The solvent viscosity  $\eta_0$  is taken to be  $\zeta C_0/\phi^2$ , which follows from  $\zeta \sim 6\pi\eta_0\xi^{-2}$ . The shear modulus is assumed to be  $G = 0.2(k_B T/v_0)\phi^3$ , from which the ratio of  $G$  to the osmotic modulus  $K_{os}$  is 0.66 in the final polymer-rich phase. The stress relaxation time is given by  $\tau = A\tau_0(\Phi^3 + 1)$  with  $A = 0.1$ . Because of this choice of  $A$ , we have  $\tau \sim \tau_0$  in early stage phase separation ( $t \lesssim 100$ ) in our simulations. As a result the viscoelasticity does not affect the patterns appreciably for  $t \lesssim 100$ , but it comes into play in later times in which  $\tau \gg \tau_0$  within polymer-rich regions. On the other hand, if  $A \geq 1$ , the viscoelasticity is crucial from the beginning and the initial stage of phase separation is

much decelerated as if there is some incubation time in accord with the experiments [2,3]. In this Letter we set  $A = 0.1$  for computational convenience. Whereas the time scale of the coarsening sensitively depends on  $A$ , the characteristic features of the late stage domain morphology are insensitive to  $A$  as long as  $\tau \gg \tau_0$  holds in late stages.

In Fig. 1 we show time evolution of patterns at  $\langle \Phi \rangle = 1.5$ , in which the polymer-rich regions are elongated droplets due to the viscoelasticity. Their shapes become circular after extremely long times. In fact, if we switch off the viscoelasticity [ $G(\phi) = 0$ ] with the other conditions held fixed, domain shapes quickly change into circular shapes due to the surface tension for  $t \geq 150$ . On the other hand, the polymer-rich regions become percolated for  $\langle \Phi \rangle \geq 1.9$  with the viscoelasticity and for  $\langle \Phi \rangle \geq 2.3$  without it for the present quench depth. Figure 2 displays patterns at  $\langle \Phi \rangle = 2$ , which closely resemble those of Tanaka. However, in the experiments desorption of solvent or the decrease of the volume fraction of the network continued for very long times, thus leading to the ultimate break-up of the network. In our case the volume fraction of the network is nearly saturated for  $t \geq 300$  and no transition to a droplet state is observed. In fact the volume fraction of the network at  $t = 500$  is only by 6% larger than the final volume fraction 0.34 at  $t \rightarrow \infty$ . At  $\langle \Phi \rangle = 2.5$  in Fig. 3 the polymer-rich domains are thicker, where the solvent droplets very slowly tend to be circular. Note that the interfaces at  $t = 150$  and 300 are mostly flat, which also occurs in phase-separating solids with elastic misfit [15].

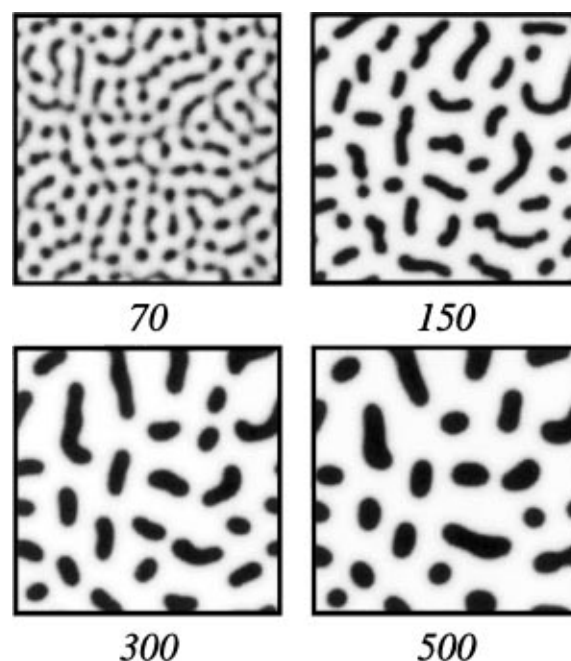


FIG. 1. Patterns of  $\Phi(x, y, t) = \phi(x, y, t)/\phi_c$  at  $\langle \Phi \rangle = 1.5$ , in which the solvent region is percolated. The numbers are the times after quenching.

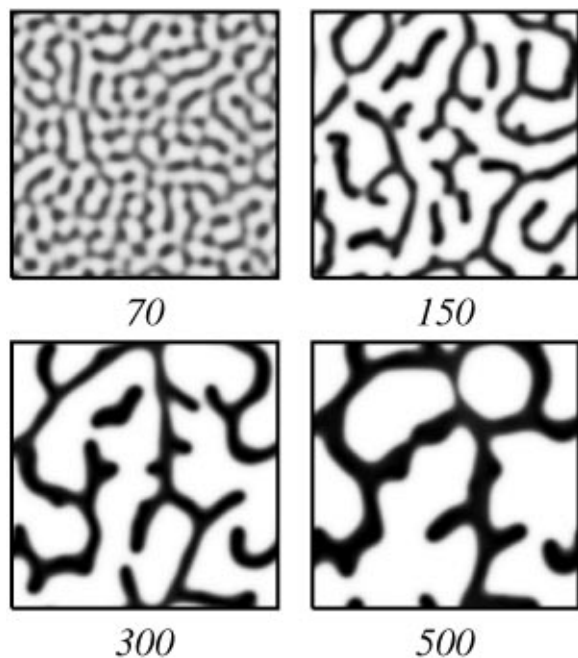


FIG. 2. Patterns of  $\Phi(x, y, t) = \phi(x, y, t)/\phi_c$  at  $\langle \Phi \rangle = 2$ . This is the case close to the boundary between the droplet and network morphologies.

In Fig. 4 we show the interface line density  $L(t)$ , which is the total perimeter length divided by the system area, at  $\langle \Phi \rangle = 2.5$  for the following three cases: (i) In the presence of viscoelasticity (bold line) we obtain  $t^{-\alpha}$  with  $\alpha \sim 1/3$  for  $t \geq 200$ . The same dynamic exponent is obtained for the other two compositions. (ii) Without viscoelasticity or for the Flory-Huggins free energy with

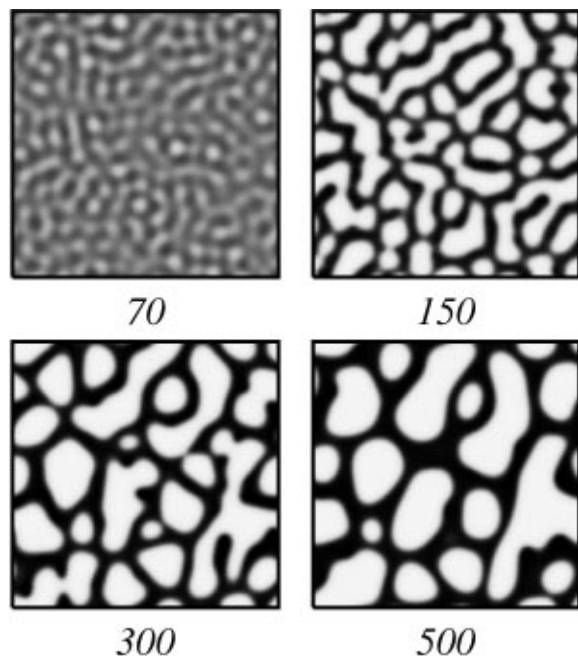


FIG. 3. Patterns of  $\Phi(x, y, t) = \phi(x, y, t)/\phi_c$  at  $\langle \Phi \rangle = 2.5$ .

hydrodynamic interaction (dotted line), the velocity field quickens the growth as  $L(t) \propto t^{-2/3}$  in the region  $100 \leq t \leq 400$ . In this case, however, solvent droplet shapes tend to be circular for  $t \geq 400$  and a crossover to the droplet growth law  $L(t) \propto t^{-1/3}$  appears to take place in later times. Notice that the growth exponent  $\frac{2}{3}$  has been obtained in the critical quench of the symmetric  $\phi^4$  model with hydrodynamic interaction in two dimensions [16]. (iii) If we remove  $\mathbf{v}$  by setting  $\mathbf{v}_p = \mathbf{w}$  in (4) in the presence of the last two terms in (6), the coarsening is slowed down from the early stage and the growth law  $L(t) \sim t^{-1/3}$  holds for  $t \geq 200$  (broken line). These results indicate that in the presence of viscoelasticity the hydrodynamic interaction is suppressed. We can see that the backbones of the network in Figs. 2 and 3 do not move as a whole and  $\mathbf{v}$  almost vanish in the network.

Then we explain why polymer-rich domains do not change their elongated shapes for such a long time in the presence of viscoelasticity. In Figure 5 we display  $W_{xx} - 1$  at  $t = 70$  and  $140$  for  $\langle \Phi \rangle = 1.5$ . In the solvent region  $\tau$  is taken to be short in (2) and  $W_{ij} \cong \delta_{ij}$ . In the early stage polymer-rich regions are elastically compressed due to desorption of solvent (as in deswelling gels). This means that  $W_{xx} - 1$  and  $W_{yy} - 1$  are negative in polymer-rich regions. Figure 5(a) shows that they are on the order of  $-0.1$  at  $t = 70$ . After a transient time, however, the surface tension force becomes effective at the ends of the stripelike polymer-rich regions, where the curvature is largest. If there were no viscoelasticity, circular domains would then appear. In our viscoelastic case, let us consider a stripe elongated along the  $y$  axis; then subsequent shape changes produce elastic expansion in the direction perpendicular to the stripe (the  $x$  axis) and elastic compression in the direction of the stripe (the  $y$  axis). Fig. 5(b) at  $t = 140$  evidently shows that  $W_{xx} - 1 > 0$  (and  $W_{yy} - 1 < 0$ ) in the stripes elongated along the  $y$  axis and vice versa for those elongated along the  $x$  axis. The resultant network stress largely cancels the stress originating from the surface tension (or that from  $\nabla\phi$ ). Thus the viscoelastic stress strongly prevents

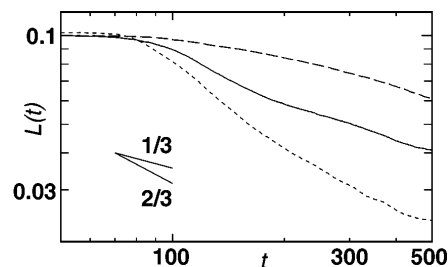


FIG. 4. Time evolution of perimeters divided by the system area at  $\langle \Phi \rangle = 2.5$ . In the bottom (dotted) curve viscoelasticity is absent and the fluid is Newtonian. The middle (bold) curve is the case of viscoelastic fluids. In the top (broken) curve  $\mathbf{v} = \phi \mathbf{v}_p + (1 - \phi) \mathbf{v}_s$  is made to vanish but the viscoelastic terms in  $\mathbf{w} = \mathbf{v}_p - \mathbf{v}_s$  are retained.

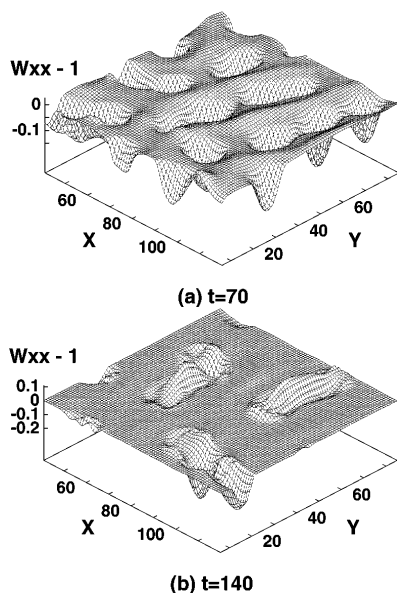


FIG. 5.  $W_{xx} - 1$  (the  $xx$  component of the strain) produced in polymer-rich regions at  $t = 70$  (a) and at  $t = 140$  (b). The region  $40 < x < 120$  and  $5 < y < 85$  is shown.

the tendency of morphology changes from elongated to circular shapes due to the surface tension. It goes without saying that the surface tension remains the driving force of coarsening because the viscoelastic stress slowly relaxes in contrast to the solid case [15].

In summary, we have examined the effects of viscoelasticity in phase-separating polymer solutions. Interestingly the network morphologies obtained here resemble those in phase-separating solid binary mixtures in the presence of elastic misfit (or when the two phases have different shear moduli) [15], although softer regions form a network in the solid case.

We thank Professor Hajime Tanaka for valuable discussions. This work is supported by the Grant-in-Aid for

Encouragement of Young Scientists, from the Ministry of Education, Science and Culture, Japan. The computation in this work has been done using the facilities of the Supercomputer Center, Institute for Solid State Physics, University of Tokyo.

- 
- [1] As experiments on polymer solutions, see, e.g., S. Nojima, K. Shiroshita, and T. Nose, *Polym. J.* **14**, 289 (1982); J. H. Aubert, *Macromolecules* **23**, 1446 (1990); J. Lal and R. Bansil, *Macromolecules* **24**, 290 (1991); N. Kuwahara and K. Kubota, *Phys. Rev. A* **45**, 7385 (1992); S. W. Song and M. Torkelson, *Macromolecules* **27**, 6390 (1994).
  - [2] H. Tanaka, *Phys. Rev. Lett.* **71**, 3158 (1993); *J. Chem. Phys.* **100**, 5253 (1994).
  - [3] H. Tanaka, *Phys. Rev. Lett.* **76**, 787 (1996).
  - [4] P. G. de Gennes, *Scaling Concepts in Polymer Physics* (Cornell University Press, Ithaca, New York, 1985), 2nd ed.
  - [5] M. Grmela, *Phys. Lett. A* **130**, 81 (1988).
  - [6] A. N. Beris and B. J. Edwards, *Thermodynamics of Flowing Systems* (Oxford University Press, Oxford, 1994).
  - [7] A. Onuki, *J. Phys. Soc. Jpn.* **59**, 3472 (1990).
  - [8] S. T. Milner, *Phys. Rev. E* **48**, 3674 (1993).
  - [9] R. B. Bird, R. C. Armstrong, and O. Hassager, *Dynamics of Polymeric Liquids* (Wiley, New York, 1987), 2nd ed., Vol. 2.
  - [10] M. Doi and A. Onuki, *J. Phys. II (France)* **2**, 1631 (1992).
  - [11] E. Helfand and H. Fredrickson, *Phys. Rev. Lett.* **62**, 2468 (1989).
  - [12] T. Tanaka, L. O. Hocker, and G. B. Benedik, *J. Chem. Phys.* **59**, 5151 (1973).
  - [13] A. Onuki, *J. Non-Cryst. Solids* **172-174**, 1151 (1994).
  - [14] G. Müller, D. Schwahn, H. Eckerlebe, J. Rieger, and T. Springer, *J. Chem. Phys.* **104**, 5826 (1996).
  - [15] A. Onuki and H. Nishimori, *Phys. Rev. B* **43**, 13 649 (1991).
  - [16] Y. Wu, F. J. Alexander, T. Lookman, and S. Chen, *Phys. Rev. Lett.* **74**, 3852 (1995); H. Furukawa (to be published).